Characterization of Analytical Phonon-Impurity Scattering Models in Complex Materials

Ramya Gurunathan[1], Riley Hanus[1], Maxwell Dylla[1], and G. Jeffrey Snyder[1]

[1]Affiliation, department, city, postcode, country
*corresponding.author@email.example

ABSTRACT

Phonon scattering off of point defects is a demonstrated mechanism to reduce the lattice thermal conductivity. The Klemens/Callaway description of point defect scattering is the most prolific analytical model. We review the essential physics of this model and compare its predictions to ab initio results of isotope scattering in Si, demonstrating the model as a useful engineering design metric. Additionally, we provide an explanation for the robustness of the model even for complex unit cell materials, which deviate considerably from a Debye model dispersion relation. We then revisit the model's application to experimental measurements of common, complex thermoelectric materials to demonstrate how the equations can be misinterpreted, leading to incomplete conclusions about the dominant scattering mechanisms.

Introduction

The use of alloys and doped materials is ubiquitous in materials science, as the electronic, optical, thermal, and structural properties of a material can be tailored through the introduction of point defects. In many applications, such as thermoelectrics, thermal barrier coatings, and microelectronics, the influence of these point defects on thermal conductivity must be understood and controlled[1–3]. The perturbation caused by point defects in a lattice can be understood as a combination of three effects: the mass contrast on the lattice site, the change in chemical bonding at the defect site, and the structural distortion of nearest neighbors around the defect[4,5]. The latter two effects are known as force constant fluctuation and strain scattering, respectively.

First-principles techniques are available to compute the perturbation induced by point defects in a lattice and the impact on thermal transport, however, multiple calculations are required to compute defect structures, evaluate scattering strengths, and solve the Boltzmann Transport Equation for the thermal conductivity[5–7]. Often, these techniques are too expensive and system dependent for routine data-fitting to determine the dominant scattering mechanisms in a system[8]. Typically, the thermal conductivity reduction due to point defect scattering is computed via analytical models, namely the Klemens/Callaway equations[4,9–11]. The equations are defined within the ostensibly limiting approximation of a single atom unit cell and the Debye model, or linear, phonon dispersion. However, by comparing to both first-principles results as well as experiment, we demonstrate the predictive quality of this model even for complex unit cell materials.

This paper provides a functional guide to understand the influence of point defects on phonon transport and apply the Callaway/Klemens equations to model thermal conductivity data. A special emphasis is placed on the extension of the model to compound materials, where the compound is approximated as a monoatomic lattice. An early discrepancy in the definition of a monoatomic lattice is identified, which has led to persisting discrepancies over how complex unit cell materials must be treated[12–17]. Additionally, the Debye model assumption in the point defect scattering equations is re-evaluated. We demonstrate a mechanism for how the model's sensitivity to dispersion relation is, in practice, lifted, justifying the use of the model in systems with arbitrary dispersion relations.

Callaway/Klemens Formulation of Point Defect Scattering

Lattice waves, or phonons, carry a substantial amount of heat through the lattice. The ability of phonons to transport heat in a material is characterized by the lattice thermal conductivity (κ). The efficiency of a phonon with frequency (ω) at transporting heat is characterized by its heat capacity (C_s), group velocity ($v_g = d\omega/dk$), and relaxation time (τ). The lattice thermal conductivity can then be expressed in terms of these values by integrating over phonon frequency up to a maximum frequency supported by the lattice (ω_{max})[9,18]. If the high temperature approximation is made, the heat capacity at frequency ω directly relates to the density of states ($g(\omega)$) as $C_s(\omega) = k_B g(\omega)$.

$$\kappa = \frac{1}{3}\int_0^{\omega_D} C_s(\omega) v_g^2 \tau(\omega) d\omega \tag{1}$$

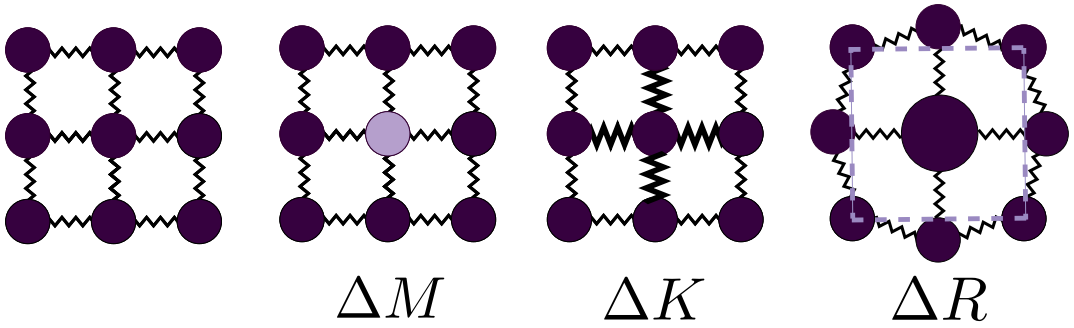

Figure 1. The lattice perturbation from a point defect is separated into three mechanisms: mass difference (ΔM), harmonic force constant difference (ΔK), and strain scattering from volume difference (ΔR).

The relaxation time of the phonons is limited by the scattering sources in the crystalline material. The three main sources of scattering are boundary scattering off of planar defects, Umklapp phonon-phonon scattering, and point defect scattering. Their associated scattering rates are summed according to Matthiessen's rules, assuming that the scattering mechanisms are uncoupled, an idea challenged in recent comparisons of these models to results from full molecular dynamics (MD) simulations[19]. The model for alloy scattering typically used to describe thermal conductivity versus alloy composition trends neglects boundary scattering to yield the total scattering rate shown in Equation 2.

$$\tau^{-1} = \tau_b^{-1} + \tau_U^{-1} + \tau_{PD}^{-1} \qquad \tau = \frac{\tau_U \tau_{PD}}{\tau_U + \tau_{PD}} \tag{2}$$

The expressions for the Umklapp and point defect inverse lifetimes, or scattering rates, take the form of $\tau_U^{-1} = B(T)\omega^2$ and $\tau_{PD}^{-1} = A\omega^4$, respectively. The scattering rate coefficients capture the relevant physics of the perturbation in the crystal lattice that induce scattering, or a transition between phonon states. The scattering rate from a static imperfection can be derived using Fermi's Golden Rule, to define the transition probability ($W_{i,j}$) from an initial to a final state. The transition probability is related to the square of the perturbation matrix element, which relates to the transition probability between to phonon states mediated by a specific perturbation to the lattice energy, and includes a lattice energy conservation criteria captured by $\delta(\Delta E)$. This transition probability is then summed over all the possible final phonon states, restricted by the conservation conditions of the phonon interaction. The collection of available final phonon states is known as the phase space.

$$W_{k,k'} = \frac{2\pi}{\hbar} \langle \mathbf{k} | H' | \mathbf{k}' \rangle^2 \delta(\Delta E) \tag{3}$$

In point defect scattering, this perturbation is attributed to three effects treated as independent scattering mechanisms: the mass difference on the defected site (ΔM), the force constant difference between the defect and its neighbors (ΔK), and the local strain or the bond distortions introduced by volume differences between the defect and host site (ΔR)[4,5,20–22] . Each of these effects perturbs a different energy contribution to the lattice Hamiltonian, and are therefore treated as independent effects. Figure provides a schematic of each of these influences. The scattering due to local strain depends on the anharmonicity of the distorted bonds, or how phonon frequencies change in response to changes initneratomic distances, as captured in the Grüneisen parameter (γ). Additionally, the strain scattering strength is scaled by the coefficient Q, which captures the number of distorted nearest neighbor bonds around a point defect. Assuming a cubic lattice with a strain field that decays with distance cubed, $Q = 4.2$, and in the case of a vacancy where bonds are missing around the defect site, $Q = 3.2$[4]. The scattering strength parameter (Γ) captures the perturbation due to each effect for a given impurity i.

$$\Gamma_i = f_i[(\frac{\Delta M_i}{\overline{M}})^2 + 2((\frac{\Delta K_i}{\overline{K}}) - 2Q\gamma(\frac{\Delta R_i}{\overline{R}}))^2] \tag{4}$$

For the point defect scattering rate (τ_{PD}^{-1}), only two phonon states, and incident and final state, are involved in the interaction. Given the conservation of energy condition, the frequencies of the final and initial phonons are equal. Therefore, the sum over all final scattering states contributes a factor of the 3D density of states sampled at the frequency of the participating phonon modes (g(ω)). Additionally, there is a factor of volume that comes from converting a sum of final $\mathbf{k}$ states to an integral over over final $\mathbf{k}$ states. The factor of volume, Ω_0, is the volume of the perturbed region[23].

$$\tau_{PD}^{-1} = \frac{\Omega_0 \pi \Gamma \omega^2 g(\omega)}{6} \qquad g(\omega) = \frac{3\omega^2}{2\pi^2 v_p^2(\omega) v_g(\omega)} \tag{5}$$

In Umklapp scattering, phonons scatter other phonons by virtue of the lattice distortions they generate. The scattering strength is, therefore, also related to the anharmonicity of the distorted bonds via the Grüneisen parameter, γ, in addition to the phase velocity of the phonon producing the distortion ($v_p(\omega) = \omega/k$) and the group velocity of the final phonon state ($v_g(\omega'')$)[23,24] Umklapp scattering is referred to as a three-phonon process because the interaction involves three phonon modes. In the typical picture, either two incident phonons combine to form a final phonon state or an initial phonon state splits to into two final phonon states. Unlike normal processes, Umklapp processes do not conserve momentum, but instead involve an exchange of momentum with the crystal lattice, which given periodicity constraints, would occur in intervals of a reciprocal lattice vector (b). The relevant conservation law is then: $k + k' = k'' + b$. An assumption is made that the magnitude of the final phonon state is small in comparison to the reciprocal lattice vector. Therefore, the final available phonon states are assumed to lie on a reciprocal space sphere with a radius equal to $\frac{1}{2}b = \frac{\pi}{a}$. The numerical prefactor of the Umklapp scattering rate varies somewhat from source to source, depending on the level of complexity assumed for the phase space[3,23,25,26].

$$\tau_U^{-1} = \frac{3\pi a \gamma^2 \omega^2 k_B}{\sqrt{2} M v_p^2(\omega) v_g(\omega'')} T \tag{6}$$

The Umklapp scattering rate appears to have the same motif present in the density of states: $\omega^2/(v_p^2 v_g)$. However, in the 3-phonon process, the frequency of the incident and final phonon state are not by necessity equivalent, and phonon velocities in this expression may be describing different phonon modes. However, if we presume that the group velocities of the initial and final phonon states due not vary considerably, the τ_U^{-1} is also approximately proportional to $g(\omega)$.

At this point it is typical to make the Debye approximation, which suggests that the v_g and v_p are independent of frequency and equal to the classical speed of sound ($v_s = d\omega/dk|_{k\to 0}$). Equation 1 for lattice thermal conductivity simplifies when substituting in the expressions for relaxation time and specific heat to the integral form of $\tan^{-1}$. Therefore, the final expression successfully used to capture thermal conductivity suppression in numerous defective systems is shown in Equation 7[10,27].

$$\frac{\kappa}{\kappa_0} = \frac{\tan^{-1} u}{u} \qquad u^2 = \frac{(6\pi^5 \Omega_0)^{1/3}}{2 k_B v_s} \Gamma \kappa_0 \tag{7}$$

Notably, the lattice thermal conductivity of the defective solid (κ_L) is normalized by the thermal conductivity of the pure solid for which the point defect scattering rate is 0 (κ_0). In typical usage of this equation, κ_0 is fit to experimental measurements and Equation 7 is used to predict the decrease in thermal conductivity with the addition of point defects.

Dispersion Relation Sensitivity

The formalism above has shown wide applicability to thermoelectric materials, which typically deviate considerably from a Debye model dispersion. We demonstrate the descriptive quality of the Callaway/Klemens (CK) expression for the case of isotope scattering in silicon, a case in which only mass difference on the defect site plays a measurable role. The data points in Figure 2 are computed using first-principles methods with lattice force constants from density functional theory, relaxation times from the T-matrix method, and finally κ_L computed using a full solution of the Boltzmann Transport Equation. In contrast, the curves are calculated from the simple analytical expression of CK theory, and show excellent correspondence. Silicon, however, is known to deviate considerably from the Debye model implicitly assumed in CK theory and so the suitability of the equations is rather surprising[28].

A study by Schrade et al. applied three dispersion relation approximations—the Debye model, a truncated Debye model, and a cubic polynomial fit—to describe the phonon structure of two half-Heusler systems. The CK κ_L curve was plotted for each case and compared to experimental curves. The study showed that the predcition of the pure thermal conductivity (κ_0) depended on the choice of dispersion. However, the shape of the curve and, therefore, the ratio κ_L/κ_0 appeared independent of the dispersion relation choice[8].

The dispersion relation dependence enters into the model through the factors of density of states and the frequency-dependent phonon velocities. In Equation 9 for lattice thermal conductivity, we rewrite the relaxation times to isolate the density of states contribution ($\tau_{PD}^{-1} = a(g(\omega))\omega^4, \tau_U^{-1} = b((g(\omega))\omega^2)$. The factor of $g(\omega)$ cancels in each of the relaxation times as well as the heat capacity.

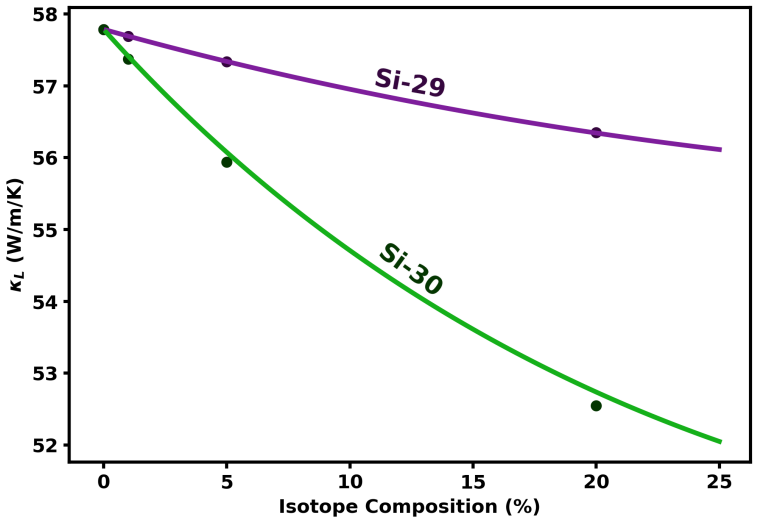

Figure 2. Silicon isotope scattering data calculated using the T-matrix method (points) and Klemens mass fluctuation model (curve)

$$\kappa = k_B \int_0^{\omega_D} v_g^2(\omega) g(\omega) \omega^2 \frac{(1/b(g(\omega)))\omega^2}{1 + a(g(\omega))\omega^2 / b(g(\omega))} d\omega \tag{8}$$

$$\kappa = \frac{k_B}{b} \int_0^{\omega_D} v_g^2(\omega) \frac{1}{1 + a/b\omega^2} d\omega \tag{9}$$

As discussed earlier, the relevant quantity is typically the ratio of the defective and pure lattice thermal conductivity (κ_L/κ_0), where κ_0 is equivalent to Equation 9 for $a = 0$. In the regimes where either $v_g^2(\omega)$ or the remaining part of the integral vary slowly with frequency, the equation can be approximated as a separable integral. Therefore, in the ratio κ_L/κ_0, the $v_g^2(\omega)$ integral would cancel.

$$\frac{\kappa_L}{\kappa_0} = \frac{\int_0^{\omega_D} v_g^2(\omega) d\omega \int_0^{\omega_D} \frac{1}{1+a/b\omega^2} d\omega}{\int_0^{\omega_D} v_g^2(\omega) d\omega} = \int_0^{\omega_D} \frac{1}{1 + a/b\omega^2} d\omega \tag{10}$$

The remainder of the integral simplifies to the $\tan^{-1}$ form shown in Equation 7. It is necessary to then consider which regimes allow for this result. The group velocity typically varies slowly with frequency at the low k-vector limit, and these long-wavelength phonons are known to dominate heat transport[13,16,17,29]. The remainder of the integral will vary slowly with frequency when the point defect coefficient (a) is small, or which is when the point defect concentration is dilute or when the perturbation induced by the point defect is small in magnitude. Therefore, at low defect concentrations, the CK model is expected to perform well. Additionally, the excellent correspondence for isotope scattering can be explained by the small magnitude of the perturbation. From this perspective, the CK model is, in practice, found to be insensitive to the chosen dispersion relation, justifying its application to complex thermoelectric materials.

Single Atom Unit Cell Approximation

The above equations have so far been defined for impurity atoms in a single element host material with one atom per unit cell, or a monatomic crystal. In extending these equations to describe defects in compound materials with potentially complex formula units, an approximation is made so that the system can be still be described as monatomic. Unfortunately, two definitions of the single atom unit cell approximation were used in early models and both have persisted in subsequent literature. In either case, the approximation is suitable given that long wavelength phonons dominate heat transport in most materials, which do not have the spatial variation to resolve the discreteness of the primitive unit cell. For simplicity, this section will focus on mass scattering alone, since this term can be understood without fitting parameters and is often invoked on its own before adding in volume-based scattering. A compound can be expressed as a combination of sublattices: $A1_{c1}A2_{c2}A3_{c3}....An_{cn}$ where Ai refers to the i$^{\text{th}}$ crystallographic sublattice and ci refers to the site degeneracy of that sublattice[30].

One interpretation, referred to as the virtual crystal approximation (VCA), defines the single atom unit cell has a virtual crystal for which each atom has the average mass ($\overline{\overline{m}}$) and average volume (V_0) of all the atoms in the compound[13]. In the VCA, parameters such as the impurity concentration, f_i, and perturbed volume, Ω_0, can be defined on a per atomic site basis, as before. The mass contrast, which factors into the calculation of Γ would be the stoichiometric average of the mass contrast on each, individual sublattice. For an example compound, $A_xB_yC_z$, the following Γ parameter is derived, and can be simplified by defining a Γ_n for each sublattice.

$$(\Delta m)^2 = \frac{x(\Delta m)_A^2 + y(\Delta m)_B^2 + z(\Delta m)_C^2}{x+y+z} \qquad \Delta m = m_i - \overline{m_A} \tag{11}$$

$$\Gamma_{vca} = f_i(\frac{\Delta M}{\overline{M}})^2 = \Gamma = \frac{x}{x+y+z}(\frac{\overline{m_A}}{\overline{m}})^2\Gamma_A + \frac{y}{x+y+z}(\frac{\overline{m_B}}{\overline{m}})^2\Gamma_B + \frac{z}{x+y+z}(\frac{\overline{m_C}}{\overline{m}})^2\Gamma_C \tag{12}$$

$$\Gamma_A = \sum_i f_i(1 - \frac{m_i}{\overline{m_A}})^2 \tag{13}$$

The second definition of the single atom unit cell, referred to as the monatomic lattice approximation (MLA), suggests that all atoms in the primitive unit cell move in phase with one another for most heat-carrying phonons[16,17,31]. Therefore, the relevant mass for the monatomic lattice is the combined mass of all atoms in the primitive unit cell, and the relevant volume per site is the entire volume of the primitive unit cell. This approximation is conceptually equivalent to treating only the acoustic phonon branches. Notably, these two interpretations imply different phonon dispersion curves for the monatomic material because their lattice parameters differ by a factor of $n^{1/3}$, where n is the number of atoms in the primitive unit cell.

Following this interpretation, we define a primitive unit cell (PUC) parameter using a statistical mechanics argument. The lattice is viewed as a sum of microstates, which represent the unit cells in the lattice. In order to calculate the overall scattering strength (Γ), we should calculate the (Γ_m) associated with each microstate in the lattice weighted by the probability (P_m) of finding that microstate in the lattice.

$$\Gamma_{mla} = \sum_m P_m\Gamma_m \tag{14}$$

In the case that impurities randomly distribute on a given sublattice, the probabilities can be calculated using the binomial distribution theorem. As an example, say there is a host compound $A_xB_yC_z$ with the impurities A', B', and C', which substitute on the A, B, and C sublattice, respectively. If f_i is the atomic site fraction of the i^{th} impurity as before, then the overall composition of the alloy is given by: $[A(1-f_a)A'(f_a)]_x[B(1-f_b)B'(f_b)]_y[C(1-f_c)C'(f_c)]_z$.

The various microstates that may compose this lattice can be defined by all the possible fillings of the A, B, and C sublattice with host atoms versus impurity atoms. Thus, each sublattice is treated as a binomial distribution in which a number of sites (set by the stoichiometry) can each have one of two outcomes: it can be occupied by an impurity atom with a probability of f_i or it can be occupied by a host atom with a probability of (1-f_i). By the binomial distribution formula, the probability that r of the total x sites on the A-sublattice will be replaced by impurity atoms is given by: $\binom{x}{r} f_A^r(1-f_A)^{x-r}$.

Now, it is possible to consider the probability of an example microstate (P_m), such as a unit cell with 2 impurity atoms on the A sublattice, 1 impurity atom on the B sublattice, and no impurity atoms on the C sublattice. This full probability would have the form below, where the shorthand $P_A(2)$ means the probability of having 2 impurity atoms on the A sublattice.

$$P_{mic} = P_A(2) * P_B(1) * P_C(0) \tag{15}$$

$$P_{mic} = [\binom{x}{2} f_A^2(1-f_A)^{x-2}] * [\binom{y}{1} f_B^1(1-f_B)^{y-1}] * [\binom{z}{0} f_C^0(1-f_C)^z] \tag{16}$$

The Γ associated with that microstate would be based on the difference between the mass of that specific microstate (M_m) and the average mass of a unit cell in the lattice. So, for the example microstate above, Γ would have the following form:

$$\Gamma = (1 - \frac{M_{mic}}{\overline{\overline{M}}})^2 \tag{17}$$

$$M_{mic} = M_A(x-2) + M_{A'}(2) + M_B(y-1) + M_{B'} + M_C(z) \tag{18}$$

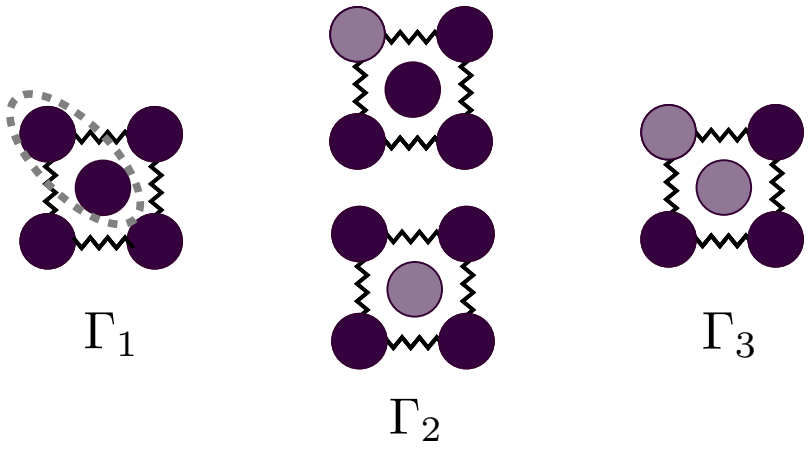

Figure 3. In an example 2-atom primitive unit cell (shown in dotted line), three possible microstates exist, containing 0,1, or 2 impurity atoms. In the unit cell basis, each microstate would bedescribed by a scattering parameter (Γ).

Now, all properties are defined on a unit cell basis, such that the relevant value of Ω_0 in the scattering rate is the volume per unit cell. When compared, these two interpretations, although highly different in their functional form and derivation, yield corresponding results. Discrepancies arise, however, when the inappropriate volume, Ω_0, is used in the calculation of the thermal conductivity. Most often, the Γ_S parameter derived by Slack is used, but the volume of the unit cell rather than the volume per atom is used to calculate thermal conductivity. The result is a large over-prediction of the point defect scattering strength. For simplicity, it is recommended to apply the virtual crystal approximation, or Equation 13 to calculate Γ_{vca}, while defining all other variables, including f_i and Ω_0, on a per atom site basis.

However, in some cases, it has been suggested that defects are associated for stability or charge counting purposes such that the composition of the unit cell is, in practice, fixed. The partially filled skutterudite system $((CeFe_4Sb_{12})_x$ $(\square Co_4Sb_{12})_{1-x})$ was suggested to form associated defects, where the filling of Ce in the structural vacancies is accompanied with Fe alloying on the Co site. In this case, a unit cell basis is recommended in order to restrict unit cell compositions to $\square Co_4Sb_{12}$ and $CeFe_4Sb_{12}$[32–34]. The thermal conductivity suppression with alloying was suggested to be describable using mass fluctuation alone, however, the volume of the unit cell was incorrectly used in conjunction with the Slack equation. The result is an over-prediction of the thermal conductivity suppression. In Figure 4, the mass fluctuation model provided in the paper is compared to the one derived here. For the "unit cell limited" case, only the $\square Co_4Sb_{12}$ and $CeFe_4Sb_{12}$ compositions have a nonzero probability of existing in the lattice. As shown, neither the standard expression nor the "limited" case suitability capture the thermal conductivity reduction, indicating that mass difference scattering is not the only κ_L reduction mechanism at play.

The overestimation of alloy scattering due to the definition of Ω_0 has also led to discrepancy over the physics of phonon vacancy scattering. Some solid solution systems incorporate stoichiometric vacancies required by the crystal structure. These vacancies have been shown to induce a large suppressions in thermal conductivity[27,31,35–40]. The perturbation introduced by a vacancy (Γ_v) involves a kinetic energy change related to the mass of a missing atom (M_a) and a potential energy change associated with the missing bond between that atom and its nearest neighbor, or -2, corresponding to twice the potential energy per atom.

$$\Gamma_v = f_v(-M_a/\overline{M} - 2)^2 \tag{19}$$

Several works fit their κ_L data without the use of the "-2" term for broken bonds, only accounting for the kinetic energy perturbation induced from missing mass. However, this is done with the misuse of the primitive unit cell volume for Ω_0. In each of the three literature examples shown in Figure 5, the mass-only scattering effect is over-predicted, however, inclusion of the broken bonds term results in a suitable fit of the thermal conductivity trend[35–37].

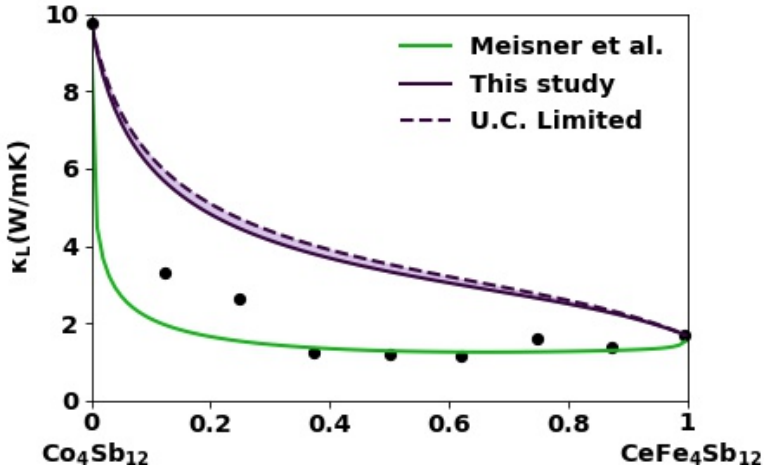

Figure 4. Thermal conductivity reduction for the filled skutterudite system[34]. Mass fluctuation model proposed in Meisner et al. (green) compared to the mass fluctuation model derived using the equations above represented by the shaded purple region. The upper bound of the shaded region represents the case for which the point defects are randomly distributed in the lattice, while the lower bound treats the fractionally filled skutterudite as a solid solution of the end members with the form: $(CeFeSb_{12})_x$ $(\square\ Co_4Sb_{12})_{1-x}$. Finally, the model with mass and volume-based scattering is plotted (dotted black).

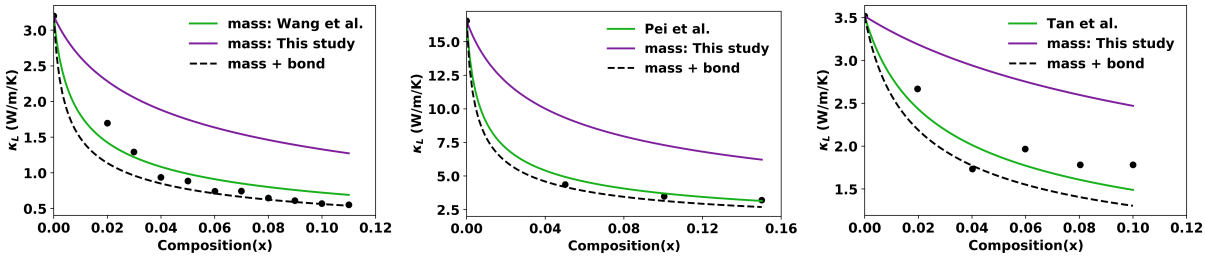

Figure 5. Thermal conductivity reductions due to vacancy scattering reported in literature. The original mass difference model (green) is compared to the mass difference model derived in this study (purple) as well as the vacancy model including both mass and bond differences (dotted black).

Conclusion

Thermal conductivity trends versus defect concentration are routinely measured to determine the dominant scattering mechanisms in a defective solid. Rapid analysis using simple, analytical expressions is, therefore, preferable to expensive, first-principles methods. The Callaway/Klemens equations reviewed are heavily utilized, but discrepancies in the inputs and uncertainty over the suitability of the approach have warranted a re-assessment of the technique. In this paper, predictions from the model are characterized against experimental and computational approaches. The model provides robust predictions for a wide range of materials, whose dispersion relations are known to deviate considerably from the Debye model. In practice, the dispersion relation dependence of the model is softened due to a cancellation of the phonon velocities in the relaxation times and heat capacity. Moreover, a review of the model usage showed a discrepancy over defining model inputs on a per unit cell or per atom basis. If model inputs are not consistently defined, the scattering parameter (Γ) will deviate by a factor of the number of atoms in the unit cell, yielding a 2-10 difference in complex thermoelectric materials.

References

1. Wan, C. L. *et al.* Effect of point defects on the thermal transport properties of (LaxGd(1-x))2Zr2O7 : Experiment and theoretical model. *Phys. Rev. B* **74**, 1–9 (2006). DOI 10.1103/PhysRevB.74.144109.
2. Wang, H., Lalonde, A. D., Pei, Y. & Snyder, G. J. The Criteria for Beneficial Disorder in Thermoelectric Solid Solutions. *Adv. Funct. Mater.* **23**, 1–11 (2012). DOI 10.1002/adfm.201201576.
3. Toberer, E. S., Zevalkink, A. & Snyder, G. J. Phonon engineering through crystal chemistry †. *J. Mater. Chem.* **21**, 15843–15852 (2011). DOI 10.1039/c1jm11754h.
4. Klemens, P. G. The Scattering of Low-Frequency Lattice Waves by Static Imperfections. *Proc. Phys. Soc* **68**, 1113 (1955).
5. Katre, A., Carrete, J., Dongre, B., Madsen, G. K. & Mingo, N. Exceptionally Strong Phonon Scattering by B Substitution in Cubic SiC. *Phys. Rev. Lett.* **119**, 1–6 (2017). DOI 10.1103/PhysRevLett.119.075902. 1703.04996.
6. Polanco, C. A. & Lindsay, L. Thermal conductivity of InN with point defects from first principles. *Phys. Rev. B* **98**, 014306 (2018). DOI 10.1103/PhysRevB.98.014306.
7. Mingo, N., Esfarjani, K., Broido, D. A. & Stewart, D. A. Cluster scattering effects on phonon conduction in graphene. *Phys. Rev. B - Condens. Matter Mater. Phys.* **81**, 1–6 (2010). DOI 10.1103/PhysRevB.81.045408.
8. Schrade, M. & Finstad, T. G. Using the Callaway Model to Deduce Relevant Phonon Scattering Processes: The Importance of Phonon Dispersion. *Phys. Status Solidi* **1800208**, 1–6 (2018). DOI 10.1002/pssb.201800208.
9. Callaway, J. Effect of Point Imperfections on Lattice Thermal Conductivity. *Phys. Rev.* **120** (1960).
10. Klemens, P. Thermal Resistance due to Point Defects at High Temperatures. *Phys. Rev.* **119**, 507–509 (1960). DOI 10.1103/PhysRev.119.507.
11. Goldsmid, H. J. Recent Studies of Bismuth Telluride and Its Alloys. *J. Appl. Phys.* **32**, 2198 (1961).
12. Slack, G. A. Effect of Isotopes on Low-Temperature Thermal Conducitivity. *Phys. Rev.* **105**, 829–831 (1957).
13. Slack, G. A. Thermal Conducitivity of MgO, Al2O3, Mg Al2O4, and Fe3O4 Crystals from 3 too 300 K. *Phys. Rev.* **126** (1962).
14. Tamura, S.-i. Isotope scattering of dispersive phonons in Ge. *Phys. Rev. B* **27** (1983).
15. Tamura, S.-i. Isotope Scattering of large wave-vector phonons in GaS and InSb: Deformation dipole and overlap-shell models. *Phyiscal Rev. B* **30**, 849–854 (1984).
16. Klemens, P. G. Thermal Resistance due to Isotopic Mass Variation. *Proc. Phys. Soc.* **70**, 833 (1957).
17. Berman, R., Foster, E. & Ziman, J. The thermal conductivity of dielectric crystals: the effect of isotopes. *R. Soc.* 344 (1956).
18. Callaway, J. Model for lattice Thermal Conductivity at Low Temperatures. *Phys. Rev.* **113**, 1046–1051 (1959). DOI 10.1103/PhysRev.113.1046. 1308.3269.
19. Feng, T., Qiu, B. & Ruan, X. Coupling between phonon-phonon and phonon-impurity scattering: A critical revisit of the spectral Matthiessen's rule. *Phys. Rev. B - Condens. Matter Mater. Phys.* **92**, 1–5 (2015). DOI 10.1103/PhysRevB.92.235206. arXiv:1512.06683v1.
20. Carruthers, P. Theory of thermal conductivity of solids at low temperatures. *Rev. Mod. Phys.* **33**, 92–138 (1961). DOI 10.1103/RevModPhys.33.92.

21. Ortiz, B. R. *et al.* Effect of extended strain fields on point defect phonon scattering in thermoelectric materials †. *Phys. Chem. Chem. Phys.* **17**, 19410–19423 (2015). DOI 10.1039/C5CP02174J.

22. Abeles, B. Lattice Thermal Conductivity of Disordered Semiconductor Alloys and High Temperatures. *Phys. Rev.* **131**, 1906–1911 (1963).

23. Berman, R. *Thermal Conduction in Solids* (Clarendon Press, Oxford, 1976).

24. Peierls, R. *Quanum Theory of Solids* (Oxford University Press, 1955).

25. Roufosse, M. & Klemens, P. Thermal Conductivity of Complex Dielectric Solids. *Phys. Rev. B* **7**, 5379–5386 (1976).

26. Parrott, J. E. *et al.* The high temperature thermal conductivity of semiconductor alloys. *Proc. Phys. Soc.* **81**, 726 (1963).

27. Zhao, M. *et al.* Defect engineering in development of low thermal conductivity materials: A review. *J. Eur. Ceram. Soc.* **37**, 1–13 (2017). DOI 10.1016/j.jeurceramsoc.2016.07.036.

28. Agne, M. T., Hanus, R. & Snyder, G. J. Minimum thermal conductivity in the context of: Diffuson -mediated thermal transport. *Energy Environ. Sci.* **11**, 609–616 (2018). DOI 10.1039/c7ee03256k.

29. Herring, C. Role of low-energy phonons in thermal conduction. *Phys. Rev.* **95**, 954–965 (1954). DOI 10.1103/PhysRev.95.954.

30. Yang, J., Meisner, G. P. & Chen, L. Strain field fluctuation effects on lattice thermal conductivity of thermoelectric compounds. *Appl. Phys. Lett.* **85**, 1140 (2004). DOI 10.1063/1.1783022.

31. Ratsifaritana, C. A. & Klemens, P. G. Scattering of phonons by vacancies. *Int. J. Thermophys.* **8**, 737–750 (1987). DOI 10.1007/BF00500791.

32. Nolas, G. & Cohn, J. Effect of partial void filling on the lattice thermal conductivity of skutterudites. *Phys. Rev. B - Condens. Matter Mater. Phys.* **58**, 164–170 (1998). DOI 10.1103/PhysRevB.58.164.

33. Wang, Y., Yang, F. & Xiao, P. Rattlers or oxygen vacancies: Determinant of high temperature plateau thermal conductivity in doped pyrochlores. *Appl. Phys. Lett.* **102**, 1–6 (2013). DOI 10.1063/1.4801319.

34. Meisner, G. P., Morelli, D. T., Hu, S., Yang, J. & Uher, C. Structure and Lattice Thermal Conductivity of Fractionally Filled Skutterudites : Solid Solutions of Fully Filled and Unfilled End Members. *Phys. Rev. Lett.* **80**, 3551–3554 (1998).

35. Tan, G. *et al.* High Thermoelectric Performance SnTe In2Te3 Solid Solutions Enabled by Resonant Levels and Strong Vacancy Phonon Scattering. *Chem. Mater.* **27**, 7801–7811 (2015). DOI 10.1021/acs.chemmater.5b03708.

36. Pei, Y. & Morelli, D. T. Vacancy phonon scattering in thermoelectric. *Appl. Phys. Lett.* **94**, 122112 (2009). DOI 10.1063/1.3109788.

37. Wang, Y. *et al.* Large Thermal Conductivity Reduction Induced by La / O Vacancies in the Thermoelectric LaCoO 3 System. *Inorg. Chem.* **50**, 4412–4416 (2011). DOI 10.1021/ic200178x.

38. Klemens, P. G. Phonon scattering by oxygen vacancies in ceramics. *Phys. B* **264**, 263–265 (1999).

39. Tan, G. *et al.* High Thermoelectric Performance in SnTe-AgSbTe2Alloys from Lattice Softening, Giant Phonon-Vacancy Scattering, and Valence Band Convergence. *ACS Energy Lett.* **3**, 705–712 (2018). DOI 10.1021/acsenergylett.8b00137.

40. Böcher, F., Culver, S. P., Peilstöcker, J., Weldert, K. S. & Zeier, W. G. *Dalt. Trans.* 3906–3914. DOI 10.1039/c7dt00381a.

Supplemental Information

0.1 Derivation of the Relaxation Times

As before, being a static perturbation, point defect scattering can be understood through Fermi's Golden Rule:

$$W_{k,k'} = \frac{2\pi}{\hbar^2} \langle \mathbf{k} | H' | \mathbf{k}' \rangle^2 \delta(\omega_k - \omega_{k'}) \tag{20}$$

The perturbation matrix Hamiltonian is similar to what it was before, but now the process involves only 2 phonons through the annihilation of one mode and creation of another.

$$\langle k | H' | k' \rangle = C(k,k') a(k) a^*(k') \tag{21}$$

Expanding the creation and annihilation operators as before, the squared perturbation Hamiltonian matrix element simplifies to:

$$\langle k | H' | k' \rangle^2 = \frac{\hbar^2}{M^2 \omega^2} C^2(k,k') [N(N'+1) - N'(N+1)] \tag{22}$$

It is shown that the term in the square brackets reduces to 1 in the integral over the constant energy surface corresponding to final $\mathbf{k}'$ states([4]).

The coefficient (C_2) will be calculated for the mass difference case, in which the perturbation stems from an atom with a mass of $M' = M_0 + \Delta M$ sitting in the primitive unit cell located at $\mathbf{R}$. The perturbation to the lattice Hamiltonian due to this mass difference can be written as:

$$E'(\mathbf{R}) = \frac{1}{2}\Delta M(\mathbf{R})\dot{u}^2(\mathbf{R}) \tag{23}$$

The Fourier transform is taken of the mass difference. Here, S refers to the number of primitive unit cells in the lattice[14,15].

$$\Delta\tilde{M}(\mathbf{Q}) = \frac{1}{S}\sum_{\mathbf{R}} \Delta M(\mathbf{R}) e^{i\mathbf{QR}} \tag{24}$$

The expression for C^2 picks up a factor of $\Delta\tilde{M}(\mathbf{Q})\Delta\tilde{M}(\mathbf{Q}')$, which is equal to:

$$\Delta\tilde{M}(\mathbf{Q})\Delta\tilde{M}(\mathbf{Q}') = \frac{1}{S^2}\sum_{\mathbf{R}} \Delta M(\mathbf{R})\Delta M(\mathbf{R}') e^{i(\mathbf{Q}'\mathbf{R}'-\mathbf{QR})} \tag{25}$$

If the approximation is then made that the point defect is randomly distributed on the lattice, the average over the squared mass difference can be taken instead. Here, S_i is the number of defected primitive unit cells and f_i is the fraction of primtive unit cells that are defective[14,15].

$$\Delta M(\mathbf{R})\Delta M(\mathbf{R}' >_{avg} =< \Delta M(\mathbf{R})^2 >_{avg} \tag{26}$$

$$\Delta\tilde{M}(\mathbf{Q})\Delta\tilde{M}(\mathbf{Q}') = \frac{1}{S}\frac{S_i}{S}\Delta M^2 = \frac{1}{S} f_i \Delta M^2 \tag{27}$$

The velocity $\dot{u}$ is again written in terms of creation and annihilation operators, which contribute a frequency dependence, such that the full expression for the coefficient C_2 is given by**?**:

$$C^2 = \frac{1}{4S} f_i (\Delta M)^2 \omega^4 \tag{28}$$

Now, scattering probability can be fully expressed as:

$$W_{k,k'} = \frac{\pi}{2S} f_i \frac{\Delta M^2}{M^2}\omega^2 \tag{29}$$

As before for Umklapp scattering, we should integrate $W_{k,k'}$ over all the possible final phonon states $\mathbf{k}'$ to get the scattering rate. This constitutes an integral over a constant energy surface or sphere of radius k in k-space. As before, the integration picks up a volume factor of $\frac{V}{2\pi^3}$, where V is the volume of the crystal (see Equations **??** and **??**). $\Omega_0 = V/S$ is the volume of the primitive unit cell.

$$\tau^{-1} = \frac{V}{(2\pi)^3}\int W_{k,k'} d^3\mathbf{k}' \tag{30}$$

$$\tau^{-1} = \frac{\Omega_0}{4\pi} f_i (\frac{\Delta M}{M})^2 \frac{\omega^4}{v_p^2(\omega) v_g(\omega)} \tag{31}$$

$$\tau^{-1} = \frac{\pi\Omega_0}{6} f_i (\frac{\Delta M}{M})^2 g(\omega)\omega^2 \tag{32}$$

0.2 Derivation of the Arctan Equation

Equation1 for lattice thermal conductivity can be simplified at the high temperature limit to the following form.

$$\kappa = \frac{k_B}{2\pi^2}\int_0^{\omega_D} \frac{\omega^2}{v_p^2(\omega)v_g(\omega)} v_g^2(\omega)\frac{\tau_U}{1+\tau_U/\tau_{PD}} d\omega \tag{33}$$

Next, the phonon velocities are pulled out of the coefficients of the relaxation times ($A = a(v_p^2 v_g)^{-1}, B = b(v_p^2 v_g)^{-1}$).

$$\kappa = \frac{k_B}{2\pi^2}\int_0^{\omega_D} v_g^2(\omega)\frac{v_g(\omega)}{v_p^2(\omega)}\omega^2 \frac{(1/b(v_p^2 v_g)^{-1})\omega^2}{1+a(v_p^2 v_g)^{-1}\omega^2/b(v_p^2 v_g)^{-1}} d\omega \tag{34}$$

The phonon velocities in the specific heat, Umklapp relaxation time, and the point defect relaxation time will cancel to yield the final simplified form.

$$\kappa = \frac{k_B}{2\pi^2 b}\int_0^{\omega_D} v_g^2(\omega)\frac{1}{1+a\omega^2/b} d\omega \tag{35}$$

If the approximation can be made that the factor of v_g^3 is largely frequency-independent, then the integral above has a solution in the form of $\tan^{-1}$.

$$\kappa = \frac{k_B v_g^2}{2\pi^2 b(b/a)^{1/2}}\tan^{-1}\left(\frac{\omega_D}{(b/a)^{1/2}}\right) \tag{36}$$